Atmospheric Research 268 (2022) 105985

Contents lists available at ScienceDirect

Atmospheric Research

journal homepage: www.elsevier.com/locate/atmosres

Integral turbulence characteristics over a clear woodland forest in northern Benin (West Africa)

Miriam Hounsinou [a,b,*], Ossénatou Mamadou [a,b,*], Maxime Wudba [c,d], Basile Kounouhewa [b], Jean-Martial Cohard [e]

[a] Institut de Mathématiques et de Sciences Physiques, Université d'Abomey-Calavi, BP 613 Dangbo, Bénin
[b] Laboratoire de Physique du Rayonnement, Faculté des Sciences et Techniques, Université d'Abomey-Calavi, Bénin
[c] Institut de Recherche pour le Développement (IRD), Bénin
[d] Université Joseph KI-ZERBO / UFR SVT, Ouagadougou, Burkina Faso
[e] Institut des Géosciences de l'Environnement, Grenoble, France

ARTICLE INFO

Keywords:
Stability
Monin-Obukhov Similarity Theory
Integral Turbulence Characteristics
Similarity Functions
Forest
West Africa

ABSTRACT

This study aims at investigating whether the Integral Turbulence Characteristics (ITC) obey the Monin-Obukhov Similarity Theory (MOST) above a forest site in a Sudanian climate, and at identifying the appropriate ITC models for this ecosystem. Data were collected from a 18 m tower equipped with an Eddy Covariance system, above the clear forest close to Bellefoungou's village, Northwest of Benin, West Africa. The turbulence intensity parameters calculated for five years and half, were analyzed according to wind speed, stability conditions and seasons. From their relationships with the stability parameter, data driven models were then obtained by the nonlinear least squares. The results showed that, all similarity functions follow MOST with a 1/3 power law whatever the stratification of the atmosphere during all the seasons excepted the temperature which had a parabolic shape in near neutral condition ($-0.05 < \zeta < 0.1$). A seasonal dependence of all ITCs was evidenced under stable conditions. We also showed that the heat transfer is relatively more efficient than H_2O transfer under both stability conditions. The established temperature and CO_2 similarity models are found to be closer, and for some given stratification conditions, to those already existing in literature. But a noteworthy finding is that the models often used to assign a quality criterion to turbulent fluxes showed an overestimation relatively to those established 'locally' for u and w through all atmospheric stratification.

1. Introduction

Understanding atmospheric turbulence is essential for evaluation of weather forecasting and atmospheric models (Honnert et al., 2011; Kalverla et al., 2016; Lee et al., 2020) and the study of pollutant dispersion (Cohan et al., 2011; Kesarkar et al., 2007) in the Atmospheric Boundary Layer (ABL). The turbulence favors exchanges of momentum, energy, and mass in the ABL, but its random behavior makes it difficult to describe (Stull, 1988). The statistical description of turbulence has been well-developed since Kolmogorov and was summarized by Stull (1988). Hence, the calculation of turbulent parameters is universal, whereas the parameterization of turbulence in numerical models still needs to be improved. For this purpose, the Monin-Obukhov Similarity Theory (MOST) is often required. This dimensional analysis links turbulent processes over a homogeneous flat surface to a single parameter universal functions that have been documented during, for example, the Kansas experiment (Businger et al., 1971), and the International Turbulence Comparison Experiment (Dyer and Bradley, 1982), under quasi-stationary atmospheric conditions, when rotational effects in the fluxes are negligible and turbulent fluxes are almost constant with altitude (Nadeau et al., 2013; Stull, 1988).

In particular, the MOST lies in expressing a relationship between the normalized standard deviations of the turbulent parameters and the atmospheric stability parameter (ζ). These normalized standard deviations are also referred to as Integral Turbulence Characteristics (ITCs) (Foken et al., 2012; Foken et al., 2004; Mauder et al., 2006). The ITCs are indeed useful to assess the quality of eddy covariance measurements (Foken et al., 2012; Foken and Wichura, 1996; Mauder et al., 2006), to estimate the ecosystem exchanges by the flux-variance method (Guo et al., 2009; Hsieh et al., 2008; Tillman, 1972) and to parameterize

* Corresponding authors at: Institut de Mathématiques et de Sciences Physiques, Université d'Abomey-Calavi, BP 613 Dangbo, Bénin.
E-mail addresses: miriam.hounsinou@imsp-uac.org (M. Hounsinou), ossenatou.mamadou@imsp-uac.org (O. Mamadou).

https://doi.org/10.1016/j.atmosres.2021.105985
Received 30 June 2021; Received in revised form 27 September 2021; Accepted 17 December 2021
Available online 27 December 2021

pollutant dispersion models (Cohan et al., 2011; Kalverla et al., 2016).

Several previous studies carried out over homogeneous flat surfaces (Businger et al., 1971), forests (Lamaud and Irvine, 2006; Padro, 1993; Rannik, 1998), inland and coastal regions (Krishnan and Kunhikrishnan, 2002; Singha and Sadr, 2012), heterogeneous ecosystems (Detto et al., 2008; Lohou et al., 2010), cities (Al-Jiboori et al., 2002; Dallman et al., 2013; Fortuniak et al., 2013) and mountains (Moraes et al., 2005; Nadeau et al., 2013) among others, have been reported in the literature. The major outcomes of these studies were that similarity functions vary according to environmental conditions leading to turbulence anisotropy and/or surface heterogeneity (Katul et al., 2013; Katul et al., 2011). In sudanian climate in the northern region of Benin (West Africa), Lohou et al. (2010) showed that in unstable conditions, the humidity turbulent characteristics at the surface are no longer driven by buoyant convection but by entrainment at the boundary layer top. However, that study remains till today, the solely performed using one year of eddy covariance data above a heterogeneous ecosystem in Benin.

Another challenge of tropical regions such as West Africa is the low wind speeds that are more frequent (Jegede et al., 1997; Krishnan and Kunhikrishnan, 2002; Yadav et al., 1996; Matthew and Ayoola, 2020). Note that the structure of turbulence in the ABL associated with low wind speeds may be different from that of strong winds (Agarwal et al., 1995). It is thus appealing to provide an adequate understanding of these turbulent parameters for this region where turbulent studies are rare compared to those carried out elsewhere in the world. This study aims at investigating the seasonal features of the integral turbulence characteristics, for stable and unstable stratifications, over an open clear woodland in the northern region of Benin (West Africa), using long-term continuous Eddy-Covariance measurements. In the present study, we 1) analyze the dependence of the integral turbulence characteristics for different seasons (dry and wet) and transitional phases (drying, moistening); 2) examine whether these relationships follow or not the MOST and build data-driven ITC models and 3) investigate the efficiency of turbulent transfer at the study site. From five years and half (June 2008 to December 2013) of in-situ eddy covariance data acquired above this ecosystem, the normalized standard deviations of the three components of wind speed and atmospheric scalars (temperature, humidity and carbon dioxide) have been computed to answer two specific questions:

- Do the relationships between these ITCs and the atmospheric stability parameter vary from season to season?
- Do the ratios obey MOST at the study site?

2. Materials and methods

2.1. Background: flux-variance similarity function

According to the Monin-Obukhov's similarity theory (MOST), the normalized standard deviations of wind speed components (u, v, w) and scalars (T, q, CO_2) are supposed to be functions of the atmospheric stability parameter (ζ). These functions are called flux-variance similarity functions or integral turbulence characteristics. Tillman (1972) was the first to use them to estimate sensible and latent heat fluxes from variances. They were later suggested by Foken and Wichura (1996) to test the development of turbulence in order to assess the quality of eddy covariance data. These functions are expressed as:

$$\frac{\sigma_x}{x_*} = \varphi(\zeta) = a_{x_1}(1 \pm b_{x_1}\zeta)^{\pm c_{x_1}} \quad (1)$$

or

$$\frac{\sigma_x}{x_*} = \varphi(\zeta) = a_{x_2} + b_{x_2}(\pm\zeta)^{\pm c_{x_2}}, \quad (2)$$

where σ_x represents the standard deviations of the variable x which can be the wind speed components or the atmospheric scalars. The coefficients $a_{x1,2}$, $b_{x1,2}$ and $c_{x1,2}$ are determ ined from the dataset herein in this study. x_* are the scaling parameters which can be respectively calculated as:

$$u_* = \sqrt{|-\overline{u'w'}|}, \quad (3)$$

$$T_* = -\frac{\overline{w'T'}}{u_*}, \quad (4)$$

$$q_* = -\frac{\overline{w'q'}}{u_*}, \quad (5)$$

$$CO_{2*} = -\frac{\overline{w'CO_2'}}{u_*}. \quad (6)$$

u', w' [m/s], T'[°C], q' [g/m^3] and CO_2' [mmol/m^3] are the fluctuations of the u, w wind speed components, temperature, absolute humidity and CO_2 respectively. $\overline{w'T'}$, $\overline{w'q'}$ and $\overline{w'co_2'}$ are respectively the covariance between the fluctuations of the vertical wind speed component and that of temperature, absolute humidity and CO_2. The atmospheric stability parameter ζ is thus given by:

$$\zeta = \frac{z - d}{L}, \quad (7)$$

where z is the measurement height, d the displacement height and L is the Obukhov length that characterizes the relation between dynamic, thermal and buoyancy processes (Foken, 2017) and is defined as:

$$L = -\frac{u_*^3\,\overline{T}}{\kappa g\,\overline{w'T'}}. \quad (8)$$

$\overline{T}$ is the virtual temperature, κ the von Karman constant and g the gravitational acceleration.

2.2. Site and instrumentation

The study was conducted at the Bellefoungou site (9.79°N, 1.72°E, 445 m), a woodland open clear forest (Fig. 1), corresponding to the most wooded savannah in term of tree density (Cotillon, 2017). Vegetation consists of an open stand of trees with crown heights of around 15 m covering 60% – 80% of the total soil area (Ago et al., 2016). A peculiar characteristic of this ecosystem is in its dominant overstory species which include *Isoberlinia tomentuosa, Isoberlinia doka, Burkea Africana and Vitellaria paradoxa* (Houéto et al., 2012; Seghieri et al., 2009).

The site is located in the Donga catchment and has a slight slope of 2.5%. The displacement height computed from Eddy covariance data using approach developed by Martano (2000), was ~7.6 m and the aerodynamic roughness length (z_0) was ~1.2 m (Mamadou, 2014). More details about the site are given by Mamadou et al. (2016).

The climate is Sudanian, characterized by a succession of wet and dry seasons separated by two transitional periods (Lothon et al., 2008; Mamadou et al., 2014). Rainfall is around 1200 mm/yr on average, falling between April and October and mean annual temperature is about 25 °C (Galle et al., 2018). Low to moderate winds characterize the site (Mamadou, 2014).

The instrumentation for the micrometeorological tower included a three-dimensional sonic anemometer (CSAT3 Campbell Sci., Logan (UT) USA) and an open path gas infrared analyzer (LI-7500, LI-COR, Lincoln (NE), USA). They were installed at 18 m above the surface and measured the three components of wind speed, sonic temperature, water vapor and carbon dioxide concentration at a 20 Hz sampling rate. Low frequency sensors for the measurement of meteorological variables such as wind speed and direction, air temperature and a complete radiative budget were also installed respectively at 18, 15 and 5 m on the tower and recorded with a 30 min time step. The rainfall was measured with a tipping-bucket rain gauge. More details on the measurement systems

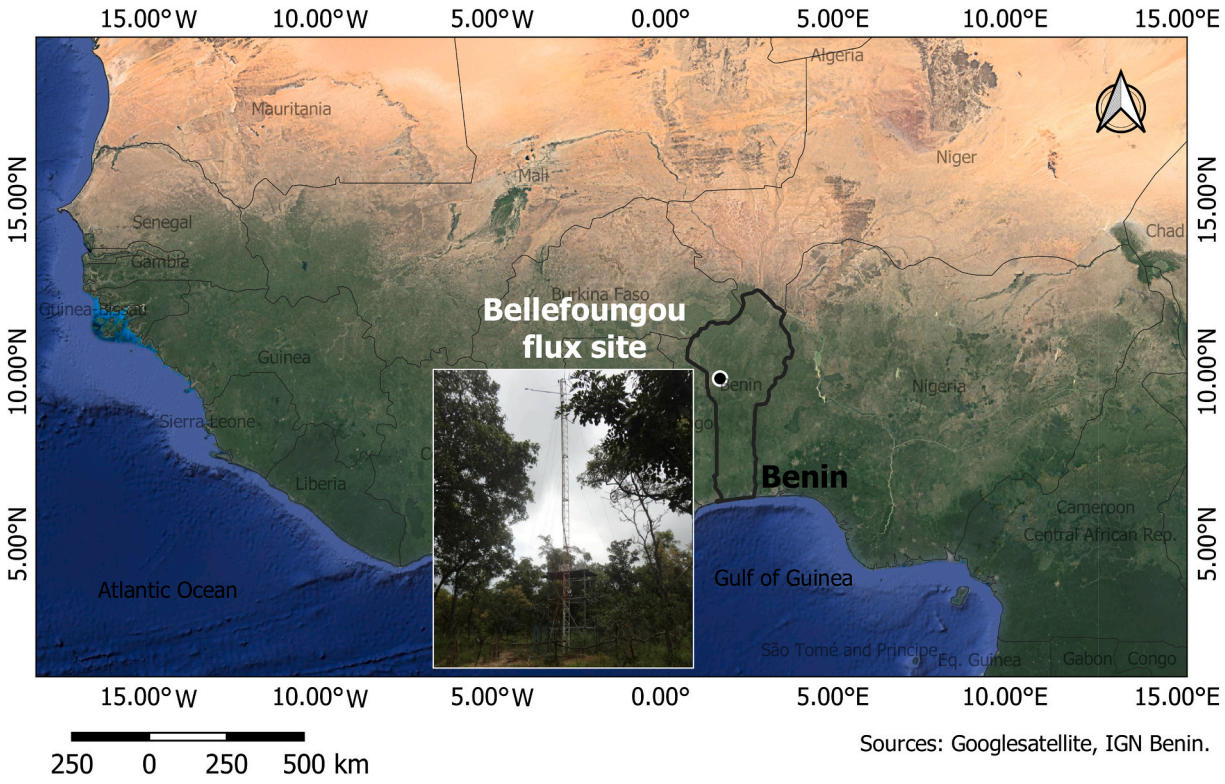

Fig. 1. Geographical location of the Bellefoungou forest site.

can be found in Mamadou et al. (2016).

2.3. Eddy covariance data processing and selection criteria

The data given in this study cover five and a half years of continuous measurements from 28th June 2008 to 31st December 2013.

Turbulent latent and sensible heat, carbon dioxide and momentum (LE, H, Fc, τ) fluxes as well as the standard deviations of wind speed components (σ_u, σ_v and σ_w [m/s]) and atmospheric scalars (σ_T [°C], σ_q [g/m^3] and σ_{CO2} [mmol/m^3]) were processed from the 20 Hz time series using the EdiRe software (Version 1.5014, R. Clement, University of Edinburgh). All the computations were performed to obtain half-hourly turbulent data and correction used following the standard procedure defined in Aubinet et al. (2000). These include de-spiking, double rotation, cross correlation for the derivation of the time lag between the sonic anemometer and the gas analyzer, density correction for the sonic temperature, spectral and Webb corrections.

Three combined criteria were used afterwards to scrutinize the 30 min data. The first was the stationarity test with a threshold of 30% according to Foken et al. (2012) and Foken and Wichura (1996). Secondly, 30 min data were deleted for both during and 30 min after rainy events. Third, $\sigma_{u,v,w,T}$ were rejected for $|H| < 10 Wm^{-2}$; σ_q were removed when $|LE| < 10 Wm^{-2}$ and σ_{CO2} were discarded during nighttime hours using a critical u_* threshold of 0.1 m.s^{-1} provided by Ago et al. (2016). For the following ITC analysis, some isolated individual peaks that were not removed with the previous selection criterions have been discarded manually from the dataset. This is also to avoid biasing the fitting of ITCs. Finally, only turbulent data for which $-2 \leq \zeta \leq 2$ have been retained for further analysis.

2.4. Computation of the integral turbulence characteristics and their corresponding models

The ITCs have been obtained as the ratios of the standard deviations of turbulent quantities, normalized with appropriate scaling flux parameters (u_*, T_*, q_* or CO_{2*}), respectively for the three wind speed components, temperature, water vapor and carbon dioxide. For the fitting of ITCs, data for which the wind speed is lower than 1 m.s^{-1} have not been taken into account. This, to avoid the cases where the turbulence is not at all developed. The remaining data were separated finally, according to the different seasons and transitional phases defined by Mamadou et al. (2014).

The Bellefoungou forest was not subjected to changes (protected woodland forest) during the years presented in this study (from June 2008 to December 2013) and no major difference in the inter-annual variability of the ITCs was observed. We therefore combined all data together and averaged them per class of 40 individual data points; separately for different seasons (dry and wet) and transitional phases (drying and moistening), and finally according to atmospheric stability conditions (unstable and stable). The number of data points of each season and per stability conditions used in this study are given in Table 1.

The models of the ITCs were determined by the nonlinear least squares method that minimizes the errors for each season. The models obtained are evaluated by using some statistical tools as the Root Mean Squared Error (RMSE), the Mean Absolute Error (MAE) and the coefficient of determination (R^2) illustrated respectively from Eqs. (9) to (11).

Table 1
Number of data retained per season under unstable and stable atmospheric conditions.

Seasons	Stratification	$\sigma_{u,v,w}/u_*$	σ_T/T_*	σ_q/q_*	σ_{CO2}/CO_{2*}
Dry	Unstable	1701	1650	789	1528
	Stable	2585	2445	1089	1511
Wet	Unstable	10967	10244	4674	9304
	Stable	7282	6787	4530	7414
Moistening	Unstable	2389	2240	1162	1120
	Stable	2203	2079	569	956
Drying	Unstable	2592	2459	1372	2277
	Stable	2460	2261	1233	1730

$$RMSE = \sqrt{\frac{1}{n}\sum_{i=1}^{n}(y_i - \hat{y}_i)^2}. \quad (9)$$

$$MAE = \frac{1}{n}\sum_{i=1}^{n}|y_i - \hat{y}_i|. \quad (10)$$

$$R^2 = 1 - \frac{\sum_{i=1}^{n}(y_i - \hat{y}_i)^2}{\sum_{i=1}^{n}(y_i - \bar{y})^2}. \quad (11)$$

With y_i the observations and $\hat{y}_i$ the data reproduced by the identified models. Wilcoxon's nonparametric statistical test was then used to check for seasonal differences at 5% (p-value < 0.05) level of significance. All the analyses were done with the software R (Rx64 3.6.1).

3. Results

3.1. Meteorological and wind conditions

The climate of the region is a Sudanian type characterized by two types of seasons (dry and wet) separated by two transitional phases (moistening and drying). This peculiar climate characteristic is driven by the Intertropical Convergence Zone's migration. The dry season is dominated by North – East (NE) Harmattan winds while the wet season is marked by South – West (SW) winds coming from the Gulf of Guinea. Wind direction and absolute humidity were combined to identify seasons at the study site as defined by Mamadou (2014); Mamadou et al. (2014).

For the years studied, total annual precipitation varied between 1017 mm and 1708 mm. The year 2013 was the driest with a total annual rainfall of 1017 mm and an average global radiation of 217 Wm^{-2}. The average annual global radiation ranged between ~187 Wm^{-2} (2008) and 218 Wm^{-2} (2011). Average daily air temperature ranged between ~18 °C and 36 °C while the average annual wind speed stayed lower than 2 m/s.

Wind speed frequency histograms for different seasons and transitional phases and according to the stratification of the atmosphere displayed in (Fig. 2a & b) showed no major difference under unstable conditions whatever the seasons. During stable conditions however, higher occurrences in higher wind speeds (2 – 3 ms^{-1}) appeared in the dry season while the remaining seasons were marked by more lower wind speeds (< 2 ms^{-1}) (Fig. 2b). This can be clearly observed on the average diurnal cycle of the wind speed (Fig. 2c).

The average diurnal course of the stability parameter shows that daytime data are characterized by unstable stratification whatever the season (~55% of total data) associated with a highest friction velocity (Fig. 2d & e). At the contrary for nighttime hours, stable stratifications were observed with a variability in terms of magnitude according to seasons. The drying period is characterized by the most stable nights, associated with more surface cooling and less atmospheric nebulosity.

3.2. Flux variance similarity functions and their seasonal variability with respect to stability and wind speed

According to the similarity theory, the normalized standard

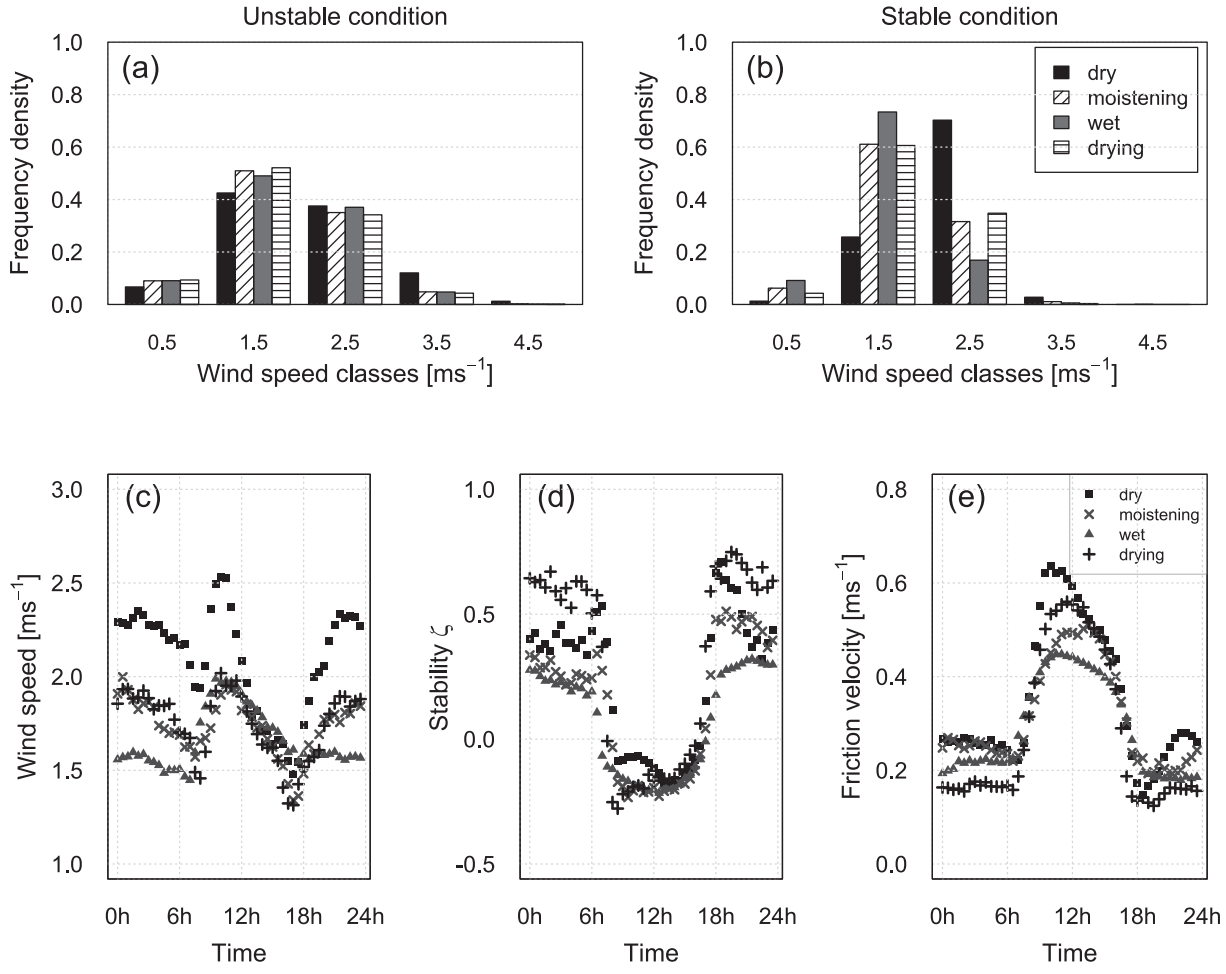

Fig. 2. Wind speed frequency density histogram (a, b) and composite diurnal cycle of: the wind speed (c), the stability parameter (d) and the friction velocity (e) at the site from the studied period during dry (black squares), wet (grey triangles), moistening (grey 'x') and drying (black '+') seasons.

deviations of turbulent parameters should be universal functions of ζ. The empirical functions and curves built for each season and stability regime from the dataset of the studied site are given in Table 2 and Figs. 3 and 4 for respectively, the wind speed components and atmospheric scalars. To help comparison between different seasons and models proposed in literature, we aggregate results of Figs. 3 and 4 on Fig. 6.

3.2.1. Normalized standard deviations of wind speed components

The similarity functions of the wind speed components obtained at the site for each season and transitional phases are in the form of Eq. (1) with $c_{x1} = 1/3$ as predicted by MOST. The coefficients a_{x1} and b_{x1} vary according to season and transitional phases (Table 2) because the ratios do not have the same distributions during different seasons (Figs. 3, 4, 6).

During unstable conditions ($\zeta < -0.1$), the ratios $\sigma_{u,v,w}/u_*$ did not vary by season. However, the Wilcoxon test performed revealed some significant differences ($0.00036 < p\text{-values} < 0.019$) between the moistening phase and the wet season for σ_u/u_* and σ_v/u_*; the two transitional phases for σ_u/u_* and finally, the dry and wet seasons for σ_v/u_*. In near neutral conditions ($0 > \zeta > -0.1$), the fitted curves showed again significant differences between seasons. The block average of the σ_u/u_* is ~1.8 in dry seasons and increases to ~2 in wet seasons as $\zeta \rightarrow 0$ (Fig. 6). The ratio σ_v/u_*, shows similar magnitude as σ_u/u_* while σ_w/u_* is on average about 1.15 in dry seasons and 1.2 in wet seasons when $-0.1 < \zeta < 0$. Furthermore, the differences in these ratios between seasons and transitional phases are not all significant when $-0.1 < \zeta < 0$. Indeed, the $\sigma_{u,w}/u_*$ ratios are not significantly different between the dry season and the drying phase. The p-value associated to the Wilcoxon test are respectively 0.85 and 0.83 for σ_u/u_* and σ_w/u_*. The seasonal variability of these normalized standard deviations of wind speed components as a function of the stability parameter are displayed in Fig. 6. The latter is indeed a combination of the blue curves in Figs. 3 and 4.

In stable conditions, the similarity functions $\sigma_{u,v,w}/u_*$ vary however according to seasons (Fig. 6). The Wilcoxon test confirms that each of the ratios σ_u/u_*, σ_v/u_* and σ_w/u_* is significantly different between dry and wet seasons with p-values << 0.05. This seasonal difference is in agreement with published literature data in West Africa (Jegede et al., 1997). The ratios σ_u/u_* and σ_v/u_* were almost two times higher than that of σ_w/u_* in all seasons. Under stable stratification, the ratio σ_w/u_* was lower than that of obtained in unstable conditions. This would suggest that for the stable conditions, stratification limits the fluctuations and differences between variabilities for horizontal and lateral wind intensities compared to the vertical one, which can be associated with anisotropy (Stiperski and Calaf, 2018). In our study, similarities between u and v variances suggest a 2-component axisymmetric anisotropy. As ζ decreases, σ_u/u_* and σ_v/u_* also decreased from ~4.5 to ~1.5. For $\zeta \sim 0$; σ_w/u_* is about 1.2 and increases with increasing stability. The ratios σ_v/u_* near neutrality tends to 2 when $\zeta \rightarrow 0$ regardless of the season (Fig. 4). This constant value of σ_v/u_* for near neutral conditions had been reported by Pahlow et al. (2001). The other normalized standard deviations of the wind speed components also vary very little under near-neutral conditions. The mean values for each season obtained when $|\zeta| < 0.05$ are presented in Table 3. The σ_u/u_* values are thought to be small compared to those obtained elsewhere (Ramana et al., 2004; Tanny et al., 2018) but are in accordance with studies conducted in regions characterized by low wind speeds (Agarwal et al., 1995; Jegede et al., 1997).

To summarize, at the studied site, the similarity functions were obviously different during dry and wet seasons when $2 > \zeta > -0.1$. However, these remained without relevant differences when $\zeta < -0.1$ for the years analyzed herein.

A variation of $\sigma_{u,v,w}/u_*$ in relation to the wind speed was also observed (Fig. 5). These ratios decrease with an increasing wind speed for all atmospheric stratification. The ratios $\sigma_{u,v}/u_*$ decrease from 8 to 2 whatever the stratification of the atmosphere while U increases from ~0.5 to ~3.5 m/s. Similarly, σ_w/u_* decreases from 4 in unstable (2.5 respectively in stable) condition to 1. According to Fig. 2b, the wind speed frequency densities in dry season were higher than those of the wet season especially for the stable stratification. These suggest that the observed seasonal differences during stable conditions could be attributed to wind speed intensities. Furthermore, the greater roughness length of the forest in the dry season than in the wet season at the study site may be another factor that can explain the seasonal dependence of turbulence characteristics. More details are given in section 4.1.

3.2.2. Normalized standard deviations of atmospheric scalars

In stable condition, the ITCs associated with atmospheric scalars are different for each season and transitional phases (p-values < 0.005) aside from, σ_q/q_* in wet season and drying phase (p-value = 0.45) and, σ_T/T_* in dry season and moistening phase (p-value = 0.58) which are not significantly different. In near neutrality ($0.01 < \zeta < 0.1$), only σ_T/T_* obtained in the drying phase showed a significant difference with the σ_T/T_* obtained in the dry and wet seasons (Fig. 6).

During unstable conditions, the similarity functions of temperature and CO_2 were independent of both wind speed (Fig. 5) and seasons (Fig. 6) but σ_{CO2}/CO_{2*} is the highest during the drying phase (Fig. 6). As for the humidity similarity functions, they were dependent on the seasons (dry and wet) but do not vary with respect to the wind speed. When comparing the σ_q/q_* functions obtained during the two transitional

Table 2
The fitting similarity functions for the normalized standard deviations of the wind components and scalars atmospheric as a function of the stability.

ITC	Stratification	Dry	Moistening	Wet	Drying
σ_u/u_*	$-2 < \zeta < -0.1$	$1.74(1 - 10.15\zeta)^{1/3}$	$1.54(1 - 17.42\zeta)^{1/3}$	$1.60(1 - 11.93\zeta)^{1/3}$	$1.80(1 - 6.43\zeta)^{1/3}$
	$-0.1 < \zeta < 0$	$1.63(1 - 13.29\zeta)^{1/3}$	$1.83(1 - 7.04\zeta)^{1/3}$	$1.91(1 - 2.96\zeta)^{1/3}$	$1.68(1 - 9.13\zeta)^{1/3}$
	$0 < \zeta < 2$	$1.59(1 + 3.78\zeta)^{1/3}$	$2.05(1 + 1.55\zeta)^{1/3}$	$1.96(1 + 3.64\zeta)^{1/3}$	$1.75(1 + 2.92\zeta)^{1/3}$
σ_v/u_*	$-2 < \zeta < -0.1$	$1.83(1 - 10.10\zeta)^{1/3}$	$1.66(1 - 13.68\zeta)^{1/3}$	$1.66(1 - 10.49\zeta)^{1/3}$	$1.94(1 - 5.29\zeta)^{1/3}$
	$-0.1 < \zeta < 0$	$2.17(1 - 1.03\zeta)^{1/3}$	$2.05(1 - 3.77\zeta)^{1/3}$	$1.97(1 - 2.38\zeta)^{1/3}$	$2.13(1 - 1.29\zeta)^{1/3}$
	$0 < \zeta < 0.1$	$2.10(1 - 1.41\zeta)^{1/3}$	$1.99(1 + 2.53\zeta)^{1/3}$	$1.94(1 + 4.89\zeta)^{1/3}$	$2.05(1 + 1.10\zeta)^{1/3}$
	$0.1 < \zeta < 2$	$1.82(1 + 2.11\zeta)^{1/3}$	$2.16(1 + 1.15\zeta)^{1/3}$	$1.95(1 + 3.88\zeta)^{1/3}$	$2.08(1 + 1.44\zeta)^{1/3}$
σ_w/u_*	$-2 < \zeta < -0.1$	$0.94(1 - 12.99\zeta)^{1/3}$	$0.95(1 - 12.15\zeta)^{1/3}$	$0.93(1 - 12.27\zeta)^{1/3}$	$0.94(1 - 11.64\zeta)^{1/3}$
	$-0.1 < \zeta < 0$	$1.11(1 - 3.13\zeta)^{1/3}$	$1.15(1 - 2.01\zeta)^{1/3}$	$1.17(1 - 1.54\zeta)^{1/3}$	$1.13(1 - 1.97\zeta)^{1/3}$
	$0 < \zeta < 0.05$	$1.10(1 + 2.74\zeta)^{1/3}$	$1.18(1 + 3.41\zeta)^{1/3}$	$1.21(1 + 3.24\zeta)^{1/3}$	$1.12(1 + 2.51\zeta)^{1/3}$
	$0.05 < \zeta < 2$	$1.14(1 + 0.73\zeta)^{1/3}$	$1.26(1 + 0.44\zeta)^{1/3}$	$1.27(1 + 0.58\zeta)^{1/3}$	$1.18(1 + 0.63\zeta)^{1/3}$
$\lvert\sigma_T/T_*\rvert$	$-2 < \zeta < -0.05$	$0.88(-\zeta)^{-1/3}$	$0.90(-\zeta)^{-1/3}$	$0.91(-\zeta)^{-1/3}$	$0.87(-\zeta)^{-1/3}$
	$-0.05 < \zeta < -0.01$	$1.56 + 0.04(-\zeta)^{-1}$	$1.40 + 0.05(-\zeta)^{-1}$	$1.81 + 0.035(-\zeta)^{-1}$	$0.94 + 0.06(-\zeta)^{-1}$
	$0.01 < \zeta < 0.1$	$2.09 + 0.04(\zeta)^{-1}$	$2.46 + 0.03(\zeta)^{-1}$	$2.40 + 0.03(\zeta)^{-1}$	$1.91 + 0.09(\zeta)^{-1}$
	$0.1 < \zeta < 2$	$2.30 + 0.81(\zeta)^{1/3}$	$2.63 + 0.32(\zeta)^{1/3}$	$2.82 - 0.21(\zeta)^{1/3}$	$2.61 + 0.52(\zeta)^{1/3}$
$\lvert\sigma_q/q_*\rvert$	$-2 < \zeta < -0.05$	$2.78(1 - 8.39\zeta)^{-1/3}$	$3.35(1 - 9.70\zeta)^{-1/3}$	$3.65(1 - 41.80\zeta)^{-1/3}$	$3.02(1 - 4.89\zeta)^{-1/3}$
	$0.05 < \zeta < 2$	$2.65(1 + 1.22\zeta)^{1/3}$	$3.94(1 - 1.13\zeta)^{1/3}$	$3.20(1 + 0.55\zeta)^{1/3}$	$3.20(1 + 0.72\zeta)^{1/3}$
$\lvert\sigma_{CO2}/CO_{2*}\rvert$	$-2 < \zeta < -0.05$	$0.91(-\zeta)^{-1/3}$	$0.88(-\zeta)^{-1/3}$	$0.93(-\zeta)^{-1/3}$	$1.06(-\zeta)^{-1/3}$
	$0.05 < \zeta < 2$	$3.47(1 + 0.46\zeta)^{1/3}$	$3.74(1 + 0.55\zeta)^{1/3}$	$3.11(1 + 0.40\zeta)^{1/3}$	$3.60(1 + 1.66\zeta)^{1/3}$

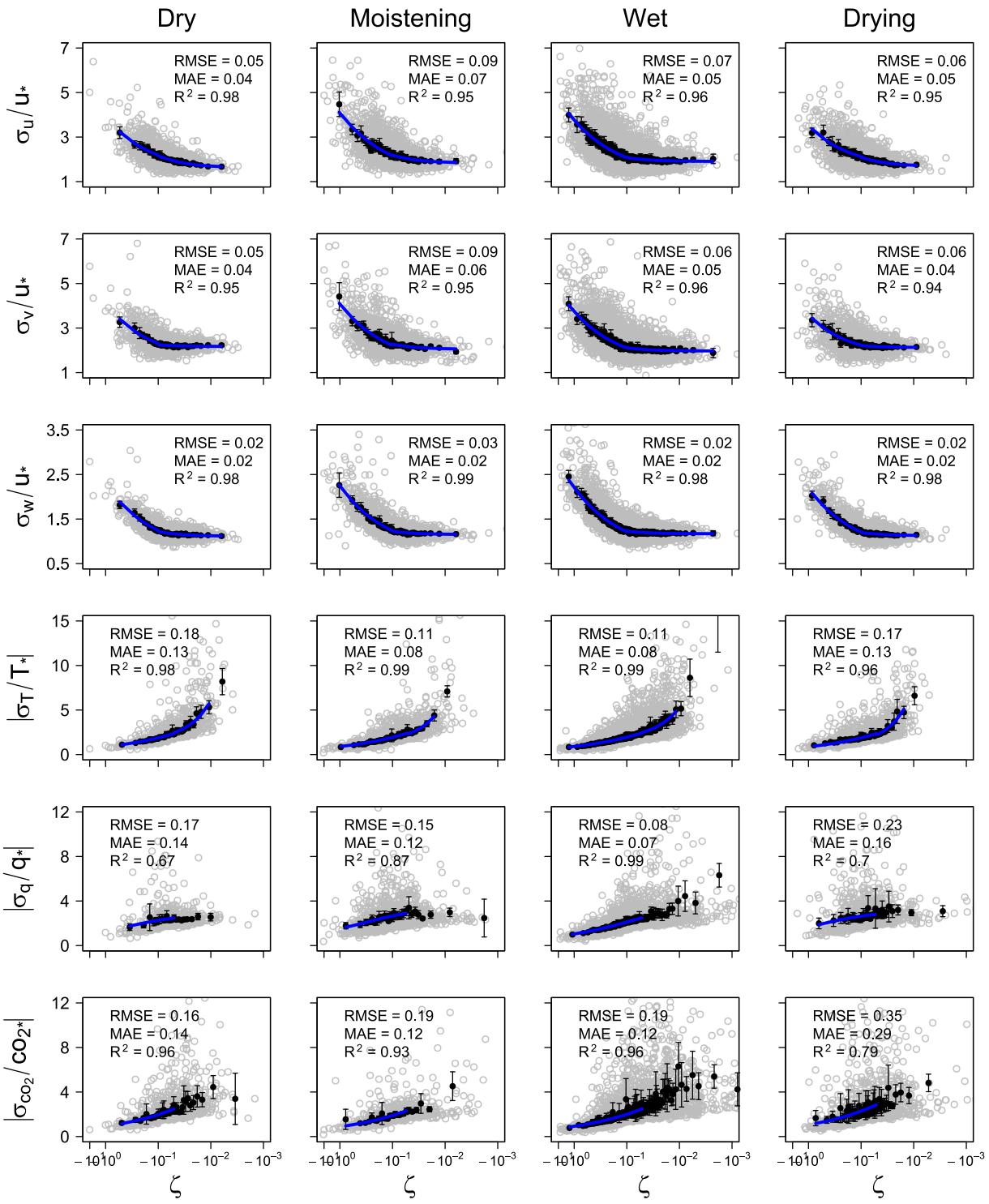

Fig. 3. Integral turbulence characteristics and their fitted curves (blue lines) for unstable atmospheric stratification during different seasons and transitional phase (grey circles). The black points represent the block average and the vertical lines represent the 95% confidence intervals on the average. (For interpretation of the references to colour in this figure legend, the reader is referred to the web version of this article.)

phases, their differences were lower (p-value = 0.29) suggesting that these ratios do not differ significantly in unstable conditions. Similar behaviors have been emphasized by Lohou et al. (2010) but for σ_T/T_* and σ_{CO2}/CO_{2*} above a heterogeneous ecosystem near the study site. A large dispersion of the turbulent humidity characteristics has however been highlighted in their study. Our results are finally in agreement with those of Ramana et al. (2004) who had shown that σ_T/T_* was almost independent of season on a flat surface whatever the stratification of the atmosphere.

The data for σ_q/q_* and σ_{CO2}/CO_{2*} when $|\zeta| < 0.05$ as well as σ_T/T_* when $|\zeta| < 0.01$ obtained over the Bellefoungou forest show nonetheless a large dispersion, so they were not included when fitting similarity functions (Figs. 3 & 4). The ITCs of the q and CO_2 exhibit similar scaling (Eq. (1)) to that of the wind speed components while σ_T/T_* which is rather defined by Eq. (2). Note that σ_{CO2}/CO_{2*} can also be expressed by the function (Eq. (2)) with $a_{x2} = 0$, in the unstable regime ($\zeta < -0.05$).

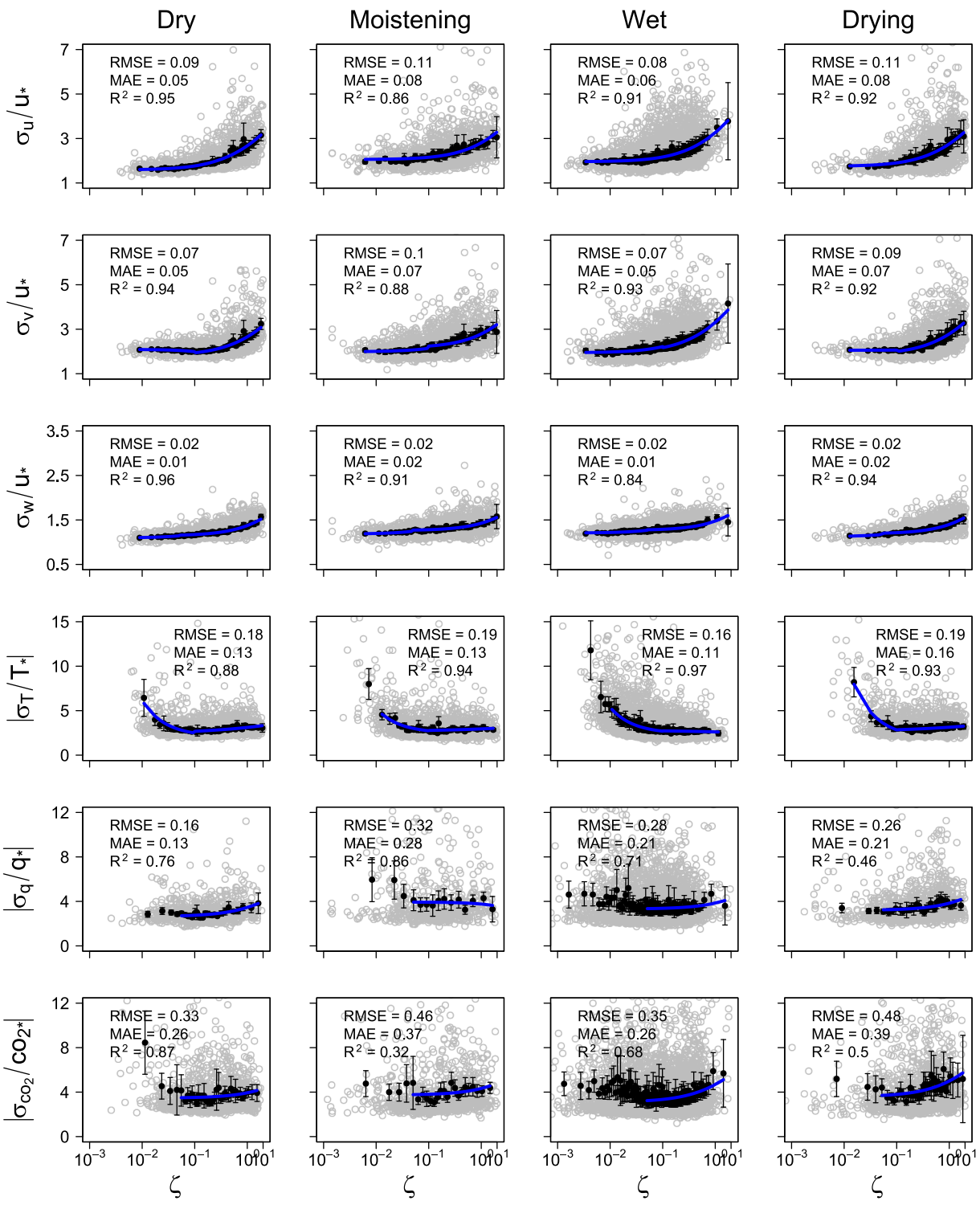

Fig. 4. Integral turbulence characteristics and their fitted curves (blue lines) for stable atmospheric stratification during different seasons and transitional phase (grey circles). The black points represent the block average and the vertical lines represent the 95% confidence intervals on the average. (For interpretation of the references to colour in this figure legend, the reader is referred to the web version of this article.)

Overall, obtained results revealed that all of these ITCs as a function of ζ (except σ_T/T_* when $-0.05 < \zeta < 0.1$), obey the MOST with a ± 1/3 power law whatever the stratification of the atmosphere, seasons and transitional phases (Figs. 3 and 4). The σ_T/T_* as a function of ζ in the near neutrality ($-0.05 < \zeta < 0.1$) range showed on the contrary a parabolic shape (Figs. 3 and 4). According to Fortuniak et al. (2013), this feature in σ_T/T_* close to the neutral stratification might be an effect of the increasing role of relative errors in the sensible heat measurements for $|\zeta| \to 0$. Similar result has been also reported by Pahlow et al. (2001) under stable conditions.

The a_{x2} coefficient of σ_T/T_* (Eq. (2)) becomes 0 when $\zeta < -0.05$ as well for $|\sigma_{CO2}/CO_{2*}|$. Considering the fact that we demonstrated that these two ratios do not show significant seasonal differences, we can therefore compute the average of b_{x2} coefficients obtained for each

Table 3
The near neutral ($|\zeta| < 0.05$) mean values and standard deviations (sd) of the $\sigma_{u,v,w}/u_*$ over the different seasons and transitional phases.

Seasons	σ_u/u_*		σ_v/u_*		σ_w/u_*	
	mean	sd	mean	sd	mean	sd
Dry	1.75	0.23	2.15	0.18	1.14	0.08
Wet	1.98	0.31	2.03	0.31	1.21	0.09
Moistening	1.98	0.30	2.08	0.29	1.20	0.09
Drying	1.82	0.25	2.14	0.21	1.15	0.09

season and transitional phases. Thus, we got $\left|\frac{\sigma_T}{T_*}\right| = 0.89(-\zeta)^{-1/3}$ for the temperature and $\left|\frac{\sigma_{CO_2}}{CO_{2*}}\right| = 0.91(-\zeta)^{-1/3}$ for the CO_2 (without taking into account $|\sigma_{CO2}/CO_{2*}|$ in the drying phase since it was significantly different (p-value $<<$ 0.05) from the moistening phase and the dry and wet seasons. By considering drying phase, $\left|\frac{\sigma_{CO_2}}{CO_{2*}}\right| = 0.94(-\zeta)^{-1/3}$. In all cases, the obtained coefficients for the temperature and CO_2 similarity functions are very close. This suggests that the turbulence characteristics of heat and CO_2 are obviously similar when $\zeta < -0.05$.

3.3. Turbulent transfer efficiency

The seasonal variability of ITCs may be also investigated with the correlation coefficients r_{wx} (Eq. (12)) and further turbulent transfer relative efficiencies (Eq. (13)) which measure the relative efficiency of heat transport compared to water vapor and carbon dioxide (McBean and Miyake, 1972).

$$r_{wx} = \frac{\overline{w'x'}}{\sigma_w \sigma_x}, \text{ with } x = u, T, q, CO_2. \tag{12}$$

$$\frac{r_{wT}}{r_{wx}} = \frac{\overline{w'T'}}{\sigma_w \sigma_T} \Big/ \frac{\overline{w'x'}}{\sigma_w \sigma_x} = \frac{\sigma_x}{x_*} \Big/ \frac{\sigma_T}{T_*}, \text{ with } x = u, q, CO_2. \tag{13}$$

The turbulent correlation coefficients obtained from data analyzed are presented in Fig. 7. The $|r_{wT}|$, $|r_{wq}|$ and $|r_{wCO2}|$ vary on average from 0.57 to 0.2; 0.50 to 0.28 and 0.55 to 0.26 respectively, when ζ varies from −2 to 0, unlike $|r_{wu}|$ which increases when approaching from unstable or stable to neutral stratification. As expected, these findings showed that heat, water vapor and CO_2 are more efficiently transported under unstable conditions than near neutral and stable conditions where the correlation coefficients are on average less than 0.35.

Under stable conditions however, all transfers especially that of water vapor and momentum, are more efficient in the dry season compared to the wet season and transitional phases. During these conditions, both $|r_{wT}/r_{wCO2}|$ and $|r_{wT}/r_{wq}| > 1$, suggesting that of heat transfer is more efficient compared to that the gases (H_2O and CO_2). But, in near neutral conditions ($|\zeta| < 0.02$), the gases transfer is a little more efficient than that of heat.

The fact that $|r_{wT}/r_{wCO2}| \simeq 1$ suggests that the heat transfer is similar to CO_2 transfer. Keeping in mind that the ITC models for the CO_2 and T were similar; this associated with the r_{wT} and r_{wCO2}, support thus the similarity of these transfers. The ($|r_{wT}/r_{wq}| \simeq 1.25$) suggests that sensible transfer is slightly higher than H_2O transfer for unstable stratification (Fig. 7). Therefore, this observed difference between H_2O and CO_2 transfers during convective conditions, may be linked to non-uniformity of H_2O sources while the absorption of CO_2 is uniformly controlled, mainly by radiation. Rannik (1998) concluded alike results

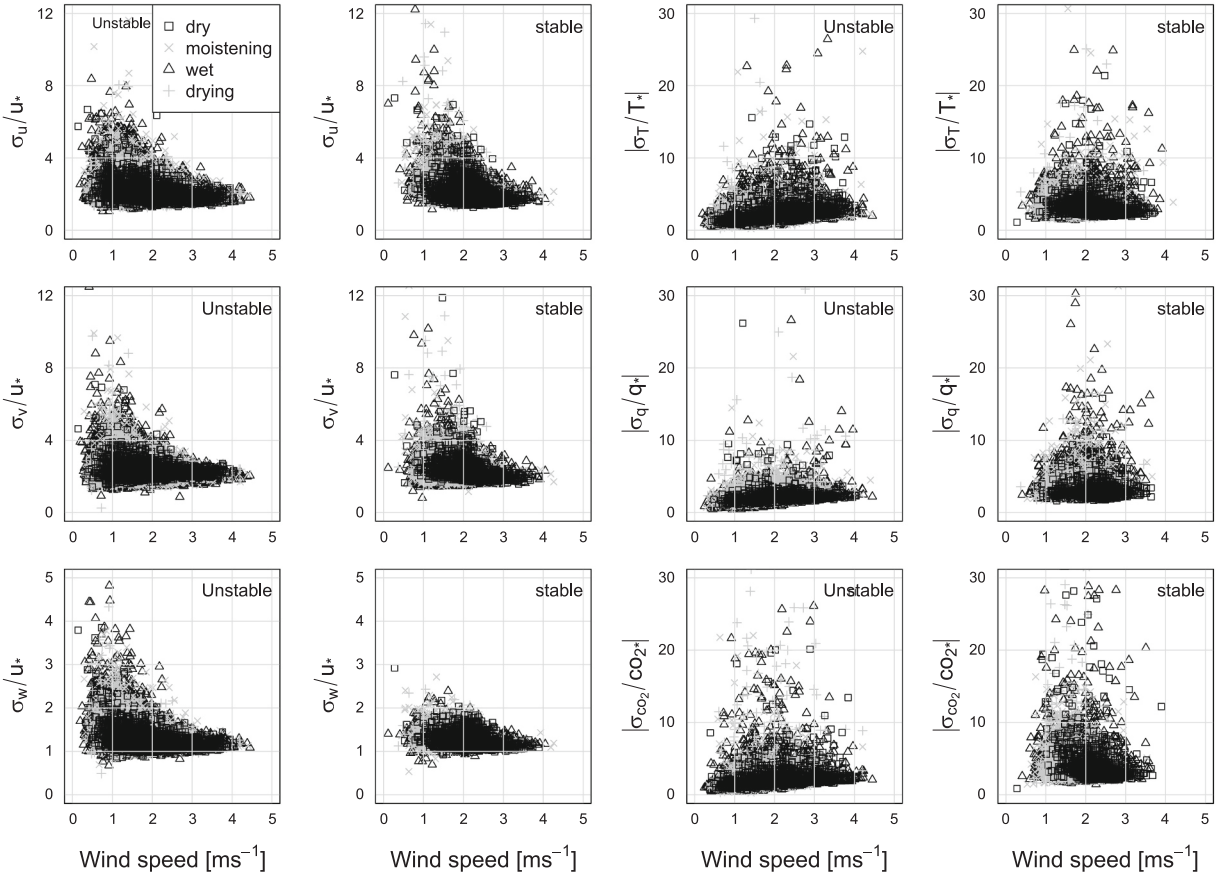

Fig. 5. Relationship between the normalized standard deviations of wind speed components and atmospheric scalars and wind speeds under unstable and stable conditions and for all seasons.

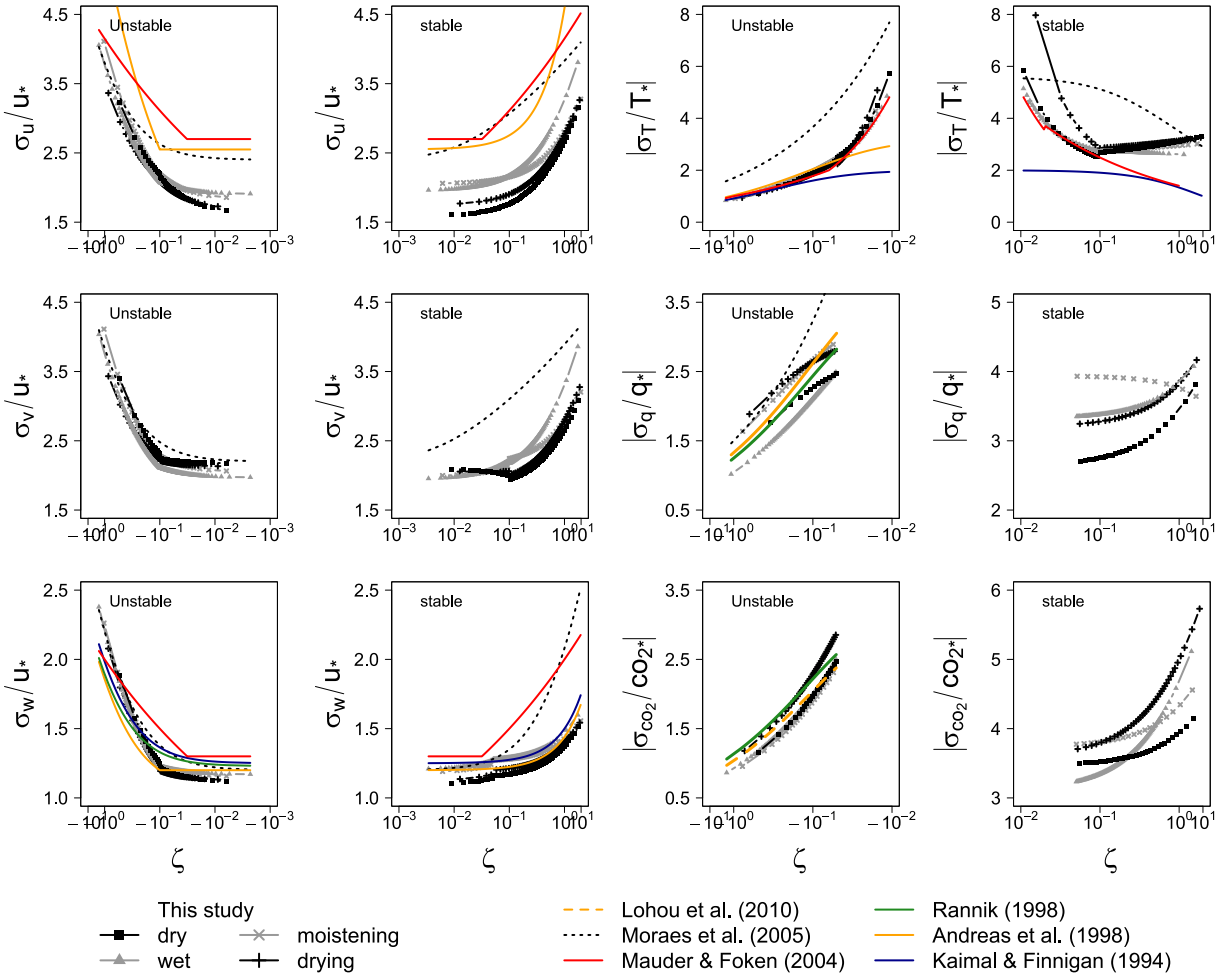

Fig. 6. The fitted curves of the integral turbulence characteristics during dry (black squares connected by lines), wet (grey triangles connected by lines), moistening (grey 'x' connected by lines) and drying (black '+' connected by lines) seasons. The literature models of Kaimal and Finnigan, 1994 (darkblue line), Rannik, 1998 (darkgreen line), Andreas et al., 1998 (orange line), Moraes et al., 2005 (black dotted line), Lohou et al., 2010 (orange dotted line) and Mauder and Foken, 2004 (red line) are also represented. (For interpretation of the references to colour in this figure legend, the reader is referred to the web version of this article.)

at a complex forest site. Overall, $|r_{wT}| > |r_{wq}|$ and $|r_{wT}| \sim |r_{wCO2}|$, confirming finally also that the temperature and CO_2 fluctuations are not affected as much as water vapor fluctuations in all conditions.

4. Discussion

4.1. Characterization of the study site

The above results indicate that the integral turbulence statistics of the three wind components and scalars (T, q and CO_2) revealed some peculiar features that are discussed here. The novelty of this study, even though this could be critical, lies in the fact that the ratios in both stable and unstable regimes have been properly examined during all seasons, and similarity functions have been drawn. A clear seasonal variation has been found which is more pronounced mainly in dry and wet seasons for stable conditions. In sudanian climate, the canopy of the vegetation shed at least 50% of their leaves but never 100% between November and February (Awessou et al., 2016; Seghieri et al., 2012; Seghieri et al., 2009). The November – February period corresponds to the dry season over the region. The fact that trees lose their leaves during the dry season (Seghieri et al., 2009) could contribute indeed to an increasing aerodynamic roughness length. This may explain the observed seasonal difference of integral turbulence characteristics $\sigma_{u,v,w}/u_*$ especially under stable conditions. Indeed, a strong aerodynamic roughness length favors more wind shear which, in turn, can lead to the development of mechanical turbulence (forced convection) during the stable stratification of the atmosphere. This, as explained by Foken (2017), is also relevant to the development of a mechanical internal boundary layer above the site of a sudden changes in the surface roughness. Indeed, mechanical internal boundary layers occur because of the different wind gradients above two surfaces, for example smooth and rough surfaces.

For the years investigated, some dispersion in the normalized standard deviations was however obtained and also reported previously on a flat surface for low wind speeds (Ramana et al., 2004). One can therefore argue that, the turbulent 'low-wind' flow properties of boundary layer processes in sudanian climate (West Africa), have been performed from this study.

When comparing dry and wet seasons and transitional phases under stable condition (Figs. 6 and 7), turbulent transfers are on average more efficient and the ratios ($\sigma_{u,v,w}/u_*$ and σ_q/q_*) are lower in the dry season. Nordbo et al. (2013) explained that the $\sigma_{u,v,w}/u_*$ are generally lower for rougher surfaces, such as the studied site. It has been also found that the sensible heat is transferred more efficiently than that of water vapor (Fig. 7). According to Detto et al. (2008); Lamaud and Irvine (2006) and Lohou et al. (2010), this is due to the dissimilarities in the source of humidity compared to that of heat. Thisbecause the variability in water vapor flux sources at the surface can enhance its variance. In addition, the fact that ($r_{wT} > r_{wq}$) depends on the relative magnitude of sensible heat and water vapor fluxes resulting mostly from the moisture state of the surface (Lamaud and Irvine, 2006).

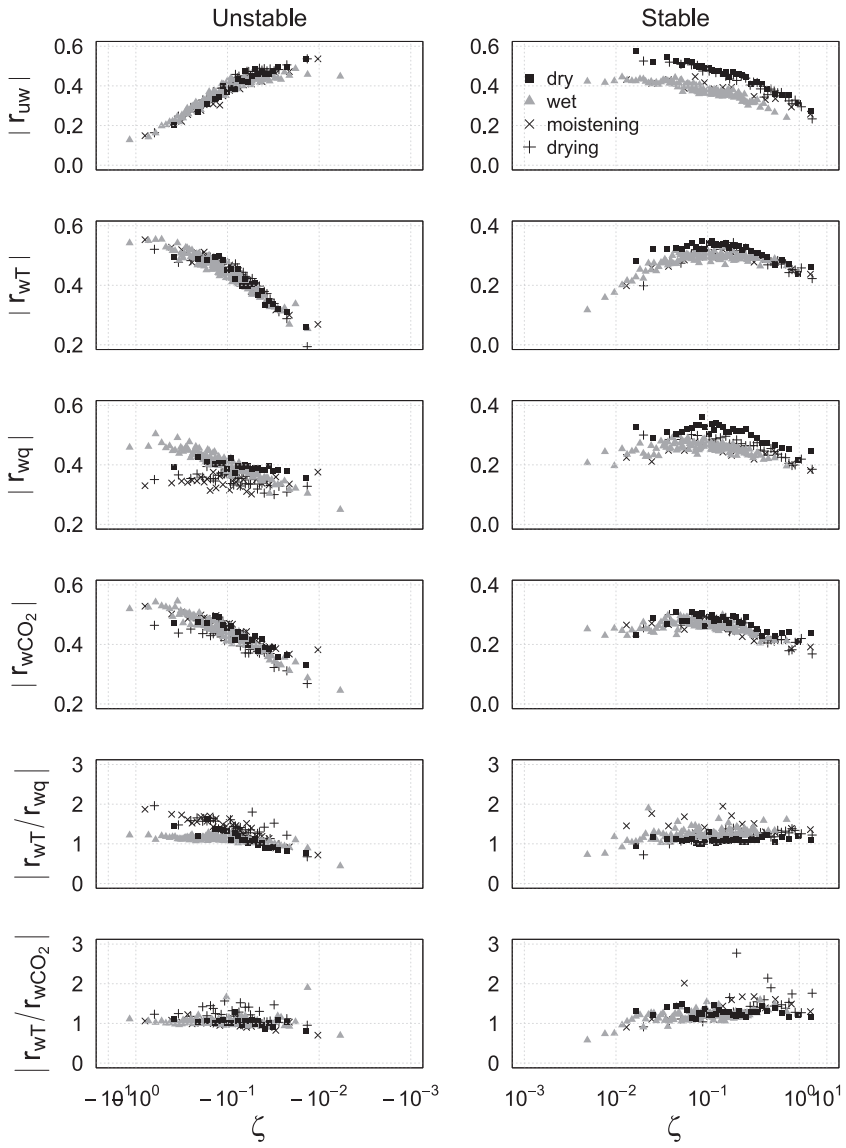

Fig. 7. The turbulent correlation coefficients r_{wx} *(x = u, T, q, CO_2)* and relative efficiency of H_2O and CO_2 with respect to temperature during dry (black squares), wet (grey triangles), moistening (grey 'x') and drying (black '+') seasons for unstable and stable conditions.

4.2. Comparison of the ITC models with others from the literature

From the authors' point of view, there are few similarity models available in the literature that reproduce clearly the observations of the study site (Fig. 6). Most of the models reported in this study here have been established on sites that are close to our study site either by vegetation, hence the models of Rannik (1998) elaborated on a forest; or by climate, hence the models of Moraes et al. (2005) developed in a tropical region and the models of Lohou et al. (2010) which are those determined by Andreas (except that of CO_2). One cannot ignore the models determined at the Kansas site (Kaimal and Finnigan, 1994), which is an ideal site for the application of MOST and the models of Foken and Wichura (1996) reviewed by Mauder and Foken (2004) which are commonly used to assess the quality of the Eddy Covariance data (Fig. 6). The majority of these models overestimate the observations of our study site.

It is also important to note that few models have been established in the literature for CO_2. Lohou et al. (2010) proposed one similarity function for CO_2 but using only the daytime (between 10 AM and 14 PM) data. This form of the similarity functions is not significantly different from those obtained from this study especially when $\zeta < -0.05$. When has the curve of the similarity function of CO_2 determined by Rannik (1998), we noticed that it was closer to the σ_{CO2}/CO_{2*} curve that we got in drying phase when $\zeta < -0.1$.

The models of σ_T/T_* determined by Foken and Wichura (1996) and revised by Mauder and Foken (2004) are in agreement with the observations of the study site under unstable conditions but under stable conditions, only the model $|\frac{\sigma_T}{T_*}| = 1.4(\zeta)^{-1/4}$ approaches the data presented in this study when $0.02 < \zeta < 0.1$. The shape of the function $|\frac{\sigma_T}{T_*}| = 0.89(-\zeta)^{-1/3}$ found above the studied ecosystem when the atmosphere is unstable ($-2 < \zeta < -0.05$) was suggested by Wyngaard et al. (1971). Foken and Wichura (1996) suggested a similar form ($|\frac{\sigma_T}{T_*}| = 1.00(-\zeta)^{-1/3}$) only for $\zeta < -1$. This indeed, was found by several authors but with slightly different coefficients. For example, Fortuniak et al. (2013); Liu et al. (2017); Wood et al. (2010) and Quan and Hu (2009); found a coefficient of 1.6; 1.25; 1.4 and 1.5 respectively.

The $\frac{\sigma_w}{u_*} = 1.25(1 + 0.2\zeta)$ function obtained from the re-examined Kansas results (Kaimal and Finnigan, 1994) and the $\frac{\sigma_w}{u_*} = 1.20(1 + 0.2\zeta)$ function proposed by Andreas et al. (1998) are near to the σ_w/u_* observed in the site when the atmosphere is stable (Fig. 6). Overall, the

models obtained from this study for the wind components are quite different from those reported in the literature. In particular, the models established by Foken and Wichura (1996) and Mauder and Foken (2004) clearly overestimate the observations at our site (Fig. 6). This mismatch could lead to the elimination of good quality eddy covariance data if one uses the models proposed by these authors to test the conditions of turbulence development. The same remarks have been emphasized previously by Fortuniak et al. (2013) for urban areas. Given the use of these similarity functions to assign a quality criterion for half-hourly turbulent fluxes, it remains relevant to check whether "local similarity functions" agree with those mostly used in the literature (Foken and Wichura, 1996; Mauder and Foken, 2004) before using them for further quality control analysis.

5. Conclusion

The aims of this work are 1) to verify whether the integral turbulence characteristics for the three wind speed components and atmospheric scalars can be described by the Monin - Obukhov similarity theory for each season and stratification regime, and 2) to determine the similarity functions for each regime, above an open clear woodland in Northern Benin (West Africa). To achieve these aims, a continuous long-term eddy covariance data has been analyzed.

The results revealed a seasonal dependence of all integral turbulence characteristics under stable condition and ITCs associated with wind speed components under near neutral conditions. The relatively lower wind speeds observed in the wet season when the atmosphere is stable resulted in relatively higher ITCs. We showed that the seasonal variability of these ITCs could be related to both the wind speed intensities and the roughness length, especially in dry season. These favor the wind shear leading probably to more dynamical turbulence. A seasonal dependence was also observed in the normalized standard deviations of humidity under unstable conditions in accordance with the result of Lohou et al. (2010). Results also suggested that turbulent transfers are less efficient in the wet season than in the dry season, especially those of momentum and water vapor under stable stratifications. The heat is similarly transferred as CO_2 when $\zeta < -0.05$; this is because radiation is the main variable governing such processes.

Although some ITCs are seasonally dependent, especially under stable conditions, all ITCs respect MOST whatever the stratification of the atmosphere, except the temperature in near neutrality. In addition, the normalized standard deviations, especially those of the atmospheric scalars, have shown some scatter, indicating some of the practical limitations of the similarity theory.

The novelty of this study, the first in the whole West African region above such an ecosystem, lies in the fact that data-driven models have been established for all wind speed components and scalars during all stability regimes. In particular, we have demonstrated a mismatch when comparing the obtained models with those often used to evaluate eddy covariance measurements. As a consequence, the use of the models established elsewhere could lead to a rejection (acceptance) of potentially good (bad) quality data. This could be investigated in further studies.

Data availability

10.17178/AMMA-CATCH.AE.H2OFlux_Odc

Author contributions

M. Hounsinou and O. Mamadou: conceptualization, formal analysis and methodology. M. Hounsinou: writing original draft. O. Mamadou., M. Hounsinou, M. Wudba, B. Kounouhewa and JM. Cohard: validation, writing-review & editing. All authors discussed the results of the manuscript.

Declaration of Competing Interest

The authors declare no conflicts of interest.

Acknowledgments

The authors are grateful to the Institute of Mathematics and Physics (IMSP) and the African Centre for Excellence in Mathematic Sciences, Informatics and Applications (ACE-MSIA) of the University of Abomey-Calavi (Bénin). M.H. was financially supported by the PhD grant provided by the 'Ministère de l'Enseignement Supérieur et de la Recherche Scientifique, Bénin' and the German Federal Ministry for Education through the German Academic Exchange Service (DAAD). The first author (M.H) is grateful to the LMI REZOC for support and assistance. This work has been supported by the prestigious fellowship from the Organization for Women in Science for the Developing World (OWSD) Early Career under the project 'Assessment of Ecosystems Exchanges in West Africa', Award agreement N°4500406717. O.M is grateful to the OWSD (https://owsd.net/) and AuthorAid (https://www.authoraid.info/en/) for assistance and help. The authors thank Marc Aubinet and the three anonymous reviewers for their fruitful and helpful comments. The AMMA-CATCH regional observation system (http://www.amma-catch.org) was set up thanks to an incentive funding of the French Ministry of Research that allowed the pooling of various pre-existing small-scale observation setups.

References

Agarwal, P., Kumar Yadav, A., Gulati, A., Raman, S., Rao, S., Singh, M.P., Nigam, S., Reddy, N., 1995. Surface layer turbulence processes in low wind speeds over land. Atmos. Environ. 29, 2089–2098. https://doi.org/10.1016/1352-2310(94)00328-I.

Ago, E.E., Agbossou, E.K., Cohard, J.M., Galle, S., Aubinet, M., 2016. Response of CO2 fluxes and productivity to water availability in two contrasting ecosystems in northern Benin (West Africa). Ann. For. Sci. 73, 483–500. https://doi.org/10.1007/s13595-016-0542-9.

Al-Jiboori, M.H., Xu, Y., Qian, Y., 2002. Local similarity relationships in the urban boundary layer. Boundary-Layer Meteorol. 102, 63–82. https://doi.org/10.1023/A:1012745322728.

Andreas, E.L., Hill, R.J., Gosz, J.R., Moore, D.I., Otto, W.D., Sarma, A.D., 1998. Statistics of surface-layer turbulence over terrain with metre-scale heterogeneity. Boundary-Layer Meteorol. 86, 379–408. https://doi.org/10.1023/A:1000609131683.

Aubinet, M., Grelle, A., Ibrom, A., Rannik, Ü., Moncrieff, J., Foken, T., Kowalski, A.S., Martin, P.H., Berbigier, P., Bernhofer, C., Clement, R., Elbers, J., Granier, A., Grünwald, T., Morgenstern, K., Pilegaard, K., Rebmann, C., Snijders, W., Valentini, R., Vesala, T., 2000. Estimates of the annual net carbon and water exchange of forests: the EUROFLUX methodology. Adv. Ecol. Res. 30, 113–175. https://doi.org/10.1016/S0065-2504(08)60018-5.

Awessou, K.G.B., Peugeot, C., Rocheteau, A., Seguis, L., Do, F.C., Galle, S., Bellanger, M., Agbossou, E., Seghieri, J., 2016. Differences in Transpiration between a Forest and an Agroforestry Tree Species in the Sudanian Belt. https://doi.org/10.1007/s10457-016-9937-8.

Businger, J.A., Wyngaard, J.C., Izumi, Y., Bradley, E.F., 1971. Flux- profile relationships in the atmospheric surface layer. J. Atmos. Sci. https://doi.org/10.1175/1520-0469(1971)028<0181:fprita>2.0.co;2.

Cohan, A., Wu, J., Dabdub, D., 2011. High-resolution pollutant transport in the San Pedro Bay of California. Atmos. Pollut. Res. 2, 237–246. https://doi.org/10.5094/APR.2011.030.

Cotillon, S.E., 2017. West Africa land use and land cover time series (No. 2017–3004, pp. 1–4). In: US Geological Survey, pp. 1–4. https://doi.org/10.3133/fs20173004.

Dallman, A., Di Sabatino, S., Fernando, H.J.S., 2013. Flow and turbulence in an industrial/suburban roughness canopy. Environ. Fluid Mech. 13, 279–307. https://doi.org/10.1007/s10652-013-9274-7.

Detto, M., Katul, G., Mancini, M., Montaldo, N., Albertson, J.D., 2008. Surface heterogeneity and its signature in higher-order scalar similarity relationships. Agric. For. Meteorol. 148, 902–916. https://doi.org/10.1016/j.agrformet.2007.12.008.

Dyer, A.J., Bradley, E.F., 1982. An alternative analysis of flux-gradient relationships at the 1976 ITCE. Boundary-Layer Meteorol. 22, 3–19. https://doi.org/10.1007/BF00128053.

Foken, T., 2017. Micrometeorology, 2nd ed. Springer-Verlag, Berlin Heidelberg, New York.

Foken, T., Wichura, B., 1996. Tools for quality assessment of surface-based flux measurements. Agric. For. Meteorol. 78, 83–105. https://doi.org/10.1016/0168-1923(95)02248-1.

Foken, T., Göckede, M., Mauder, M., Mahrt, L., Amiro, B., Munger, W., 2004. Post-field data quality control. In: Handbook of Micrometeorology, pp. 181–208.

Foken, T., Leuning, R., Oncley, S.R., Mauder, M., Aubinet, M., 2012. Corrections and data quality control. In: Eddy Covariance, pp. 85–131. https://doi.org/10.1007/978-94-007-2351-1.

Fortuniak, K., Pawlak, W., Siedlecki, M., 2013. Integral turbulence statistics over a central European City centre. Boundary-Layer Meteorol. 146, 257–276. https://doi.org/10.1007/s10546-012-9762-1.

Galle, S., Grippa, M., Peugeot, C., Moussa, I.B., Cappelaere, B., Demarty, J., Mougin, E., Panthou, G., Adjomayi, P., Agbossou, E.K., Ba, A., Boucher, M., Cohard, J.-M., Descloitres, M., Descroix, L., Diawara, M., Dossou, M., Favreau, G., Gangneron, F., Gosset, M., Hector, B., Hiernaux, P., Issoufou, B.-A., Kergoat, L., Lawin, E., Lebel, T., Legchenko, A., Abdou, M.M., Malam-Issa, O., Mamadou, O., Nazoumou, Y., Pellarin, T., Quantin, G., Sambou, B., Seghieri, J., Séguis, L., Vandervaere, J.-P., Vischel, T., Vouillamoz, J.-M., Zannou, A., Afouda, S., Alhassane, A., Arjounin, M., Barral, H., Biron, R., Cazenave, F., Chaffard, V., Chazarin, J.-P., Guyard, H., Koné, A., Mainassara, I., Mamane, A., Oi, M., Ouani, T., Soumaguel, N., Wubda, M., Ago, E.E., Alle, I.C., Allies, A., Arpin-Pont, F., Awessou, B., Cassé, C., Charvet, G., Dardel, C., Depeyre, A., Diallo, F.B., Do, T., Fatras, C., Frappart, F., Gal, L., Gascon, T., Gibon, F., Guiro, I., Ingatan, A., Kempf, J., Kotchoni, D.O.V., Lawson, F.M.A., Leauthaud, C., Louvet, S., Mason, E., Nguyen, C.C., Perrimond, B., Pierre, C., Richard, A., Robert, E., Román-Cascón, C., Velluet, C., Wilcox, C., 2018. AMMA-CATCH, a critical zone observatory in West Africa monitoring a region in transition. Vadose Zone J. 17, 180062 https://doi.org/10.2136/vzj2018.03.0062.

Guo, X., Zhang, H., Cai, X., Kang, L., Zhu, T., Leclerc, M.Y., 2009. Flux-Variance Method for Latent Heat and Carbon Dioxide Fluxes in Unstable Conditions, pp. 363–384. https://doi.org/10.1007/s10546-009-9377-3.

Honnert, R., Masson, V., Couvreux, F., 2011. A diagnostic for evaluating the representation of turbulence in atmospheric models at the kilometric scale. J. Atmos. Sci. 68, 3112–3131. https://doi.org/10.1175/JAS-D-11-061.1.

Houéto, G., Fandohan, B., Ouédraogo, A., Ago, E.E., Salako, V.K., Assogbadjo, A.E., Kakaï, R.G., Sinsina, B., 2012. Floristic and dendrometric analysis of woodlands in the Sudano-Guinean zone: a case study of Belléfoungou forest reserve in Benin. Acta Bot. Gall. 159, 387–394. https://doi.org/10.1080/12538078.2012.735124.

Hsieh, C.I., Lai, M.C., Hsia, Y.J., Chang, T.J., 2008. Estimation of sensible heat, water vapor, and CO2 fluxes using the flux-variance method. Int. J. Biometeorol. 52, 521–533. https://doi.org/10.1007/s00484-008-0149-4.

Jegede, O., Fasheun, T.A., Adeyefa, Z.D., Balogun, A.A., 1997. The effect of atmospheric stability on the surface-layer characteristics in a low-wind area of tropical West Africa research note. Boundary-Layer Meteorol. 85, 309–323. https://doi.org/10.1023/A:1000447600185.

Kaimal, J.C., Finnigan, J.J., 1994. Atmospheric Boundary Layer Flows: Their Structure and Measurement. Oxford University Press, New York.

Kalverla, P.C., Duine, G.J., Steeneveld, G.J., Hedde, T., 2016. Evaluation of the weather research and forecasting model in the durance valley complex terrain during the KASCADE field campaign. J. Appl. Meteorol. Climatol. 55, 861–882. https://doi.org/10.1175/JAMC-D-15-0258.1.

Katul, G.G., Konings, A.G., Porporato, A., 2011. Mean velocity profile in a sheared and thermally stratified atmospheric boundary layer. Phys. Rev. Lett. 107 https://doi.org/10.1103/PhysRevLett.107.268502.

Katul, G.G., Li, D., Chameki, M., Bou-Zeid, E., 2013. Mean scalar concentration profile in a sheared and thermally stratified atmospheric surface layer. Phys. Rev. E 87. https://doi.org/10.1103/PhysRevE.87.023004.

Kesarkar, A.P., Dalvi, M., Kaginalkar, A., Ojha, A., 2007. Coupling of the weather research and forecasting model with AERMOD for pollutant dispersion modeling. A case study for PM10 dispersion over Pune, India. Atmos. Environ. 41, 1976–1988. https://doi.org/10.1016/j.atmosenv.2006.10.042.

Krishnan, P., Kunhikrishnan, P.K., 2002. Some characteristics of atmospheric surface layer over a tropical inland region during southwest monsoon period. Atmos. Res. 62, 111–124. https://doi.org/10.1016/S0169-8095(02)00004-2.

Lamaud, E., Irvine, M., 2006. Temperature-humidity dissimilarity and heat-to-water-vapour transport efficiency above and within a pine forest canopy: the role of the Bowen ratio. Boundary-Layer Meteorol. 120, 87–109. https://doi.org/10.1007/s10546-005-9032-6.

Lee, J., Hong, J., Noh, Y., Jiménez, P.A., 2020. Implementation of a roughness sublayer parameterization in the Weather Research and forecasting model (WRF version 3.7.1) and its evaluation for regional climate simulations. Geosci. Model Dev. 13, 521–536. https://doi.org/10.5194/gmd-13-521-2020.

Liu, Y., Liu, H.Z., Wang, L., 2017. The vertical distribution characteristics of integral turbulence statistics in the atmospheric boundary layer over an urban area in Beijing. Sci. China Earth Sci. 60, 1533–1545. https://doi.org/10.1007/s11430-016-9050-5.

Lohou, F., Saïd, F., Lothon, M., Durand, P., Serça, D., 2010. Impact of boundary-layer processes on near-surface turbulence within the West African monsoon. Boundary-Layer Meteorol. 136, 1–23. https://doi.org/10.1007/s10546-010-9493-0.

Lothon, M., Saïd, F., Lohou, F., Campistron, B., 2008. Observation of the diurnal cycle in the low troposphere of West Africa. Mon. Weather Rev. 136, 3477–3500. https://doi.org/10.1175/2008MWR2427.1.

Mamadou, O., 2014. Etude des Flux d'Evapotranspiration en Climat Soudanien: Comportement Comparé de Deux Couverts Végétaux au Bénin. Université de Grenoble (France) et Université d'Abomey-Calavi (Bénin), Abomey-Calavi.

Mamadou, O., Cohard, J.M., Galle, S., Awanou, C.N., Diedhiou, A., Kounouhewa, B., Peugeot, C., 2014. Energy fluxes and surface characteristics over a cultivated area in Benin: Daily and seasonal dynamics. Hydrol. Earth Syst. Sci. 18, 893–914. https://doi.org/10.5194/hess-18-893-2014.

Mamadou, O., Galle, S., Cohard, J.M., Peugeot, C., Kounouhewa, B., Biron, R., Hector, B., Zannou, A.B., 2016. Dynamics of water vapor and energy exchanges above two contrasting Sudanian climate ecosystems in Northern Benin (West Africa). J. Geophys. Res. 121, 11269–11286. https://doi.org/10.1002/2016JD024749.

Martano, P., 2000. Estimation of surface roughness length and displacement height from single-level sonic anemometer data. J. Appl. Meteorol. 39, 708–715. https://doi.org/10.1175/1520-0450(2000)039<0708:EOSRLA>2.0.CO;2.

Matthew, O.J., Ayoola, M.A., 2020. Seasonality of wind speed, wind shears and precipitation over West Africa. J. Atmos. Solar-Terrestrial Phys. 207, 105371 https://doi.org/10.1016/j.jastp.2020.105371.

Mauder, M., Foken, T., 2004. Documentation and instruction manual of the eddy-covariance software package TK3. Arbeitsergebnisse 60 (ISSN 1614-8916).

Mauder, M., Liebethal, C., Göckede, M., Leps, J.P., Beyrich, F., Foken, T., 2006. Processing and quality control of flux data during LITFASS-2003. Boundary-Layer Meteorol. 121, 67–88. https://doi.org/10.1007/s10546-006-9094-0.

McBean, G.A., Miyake, M., 1972. Turbulent transfer mechanisms in the atmospheric surface layer. Q. J. R. Meteorol. Soc. 98, 383–398. https://doi.org/10.1002/qj.49709841610.

Moraes, O.L.L., Acevedo, O.C., Degrazia, G.A., Anfossi, D., Da Silva, R., Anabor, V., 2005. Surface layer turbulence parameters over a complex terrain. Atmos. Environ. 39, 3103–3112. https://doi.org/10.1016/j.atmosenv.2005.01.046.

Nadeau, D.F., Pardyjak, E.R., Higgins, C.W., Parlange, M.B., 2013. Similarity scaling over a steep alpine slope. Boundary-Layer Meteorol. 147, 401–419. https://doi.org/10.1007/s10546-012-9787-5.

Nordbo, A., Järvi, L., Haapanala, S., Moilanen, J., Vesala, T., 2013. Intra-city variation in urban morphology and turbulence structure in Helsinki, Finland. Boundary-Layer Meteorol. 146, 469–496. https://doi.org/10.1007/s10546-012-9773-y.

Padro, J., 1993. An investigation of flux-variance methods and universal functions applied to three land-use types in unstable conditions. Boundary-Layer Meteorol. 66, 413–425. https://doi.org/10.1007/BF00712731.

Pahlow, M., Parlange, M.B., Porté-Agel, F., 2001. On Monin–Obukhov Similarity in the Stable Atmospheric Boundary Layer. https://doi.org/10.1023/A:1018909000098.

Quan, L., Hu, F., 2009. Relationship between turbulent flux and variance in the urban canopy. Meteorog. Atmos. Phys. 104, 29–36. https://doi.org/10.1007/s00703-008-0012-5.

Ramana, M.V., Krishnan, P., Kunhikrishnan, P.K., 2004. Surface boundary-layer characteristics over a tropical inland station: Seasonal features. Boundary-Layer Meteorol. 111, 153–175. https://doi.org/10.1023/B:BOUN.0000010999.25921.1a.

Rannik, Ü., 1998. On the surface layer similarity at a complex forest site. J. Geophys. Res. Atmos. 103, 8685–8697. https://doi.org/10.1029/98JD00086.

Seghieri, J., Vescovo, A., Padel, K., Soubie, R., Arjounin, M., Boulain, N., de Rosnay, P., Galle, S., Gosset, M., Mouctar, A.H., Peugeot, C., Timouk, F., 2009. Relationships between climate, soil moisture and phenology of the woody cover in two sites located along the West African latitudinal gradient. J. Hydrol. 375, 78–89. https://doi.org/10.1016/j.jhydrol.2009.01.023.

Seghieri, J., Carreau, J., Boulain, N., De Rosnay, P., Arjounin, M., Timouk, F., 2012. Is Water Availability Really the Main Environmental Factor Controlling the Phenology of Woody Vegetation in the Central Sahel ?, pp. 861–870. https://doi.org/10.1007/s11258-012-0048-y.

Singha, A., Sadr, R., 2012. Characteristics of surface layer turbulence in coastal area of Qatar. Environ. Fluid Mech. 12, 515–531. https://doi.org/10.1007/s10652-012-9242-7.

Stiperski, I., Calaf, M., 2018. Dependence of near-surface similarity scaling on the anisotropy of atmospheric turbulence. Q. J. R. Meteorol. Soc. 144, 641–657. https://doi.org/10.1002/qj.3224.

Stull, R.B., 1988. An Introduction to Boundary Layer Meteorology. https://doi.org/10.1007/978-94-009-3027-8.

Tanny, J., Lukyanov, V., Neiman, M., Cohen, S., Teitel, M., Seginer, I., 2018. Energy balance and partitioning and vertical profiles of turbulence characteristics during initial growth of a banana plantation in a screenhouse. Agric. For. Meteorol. 256–257, 53–60. https://doi.org/10.1016/j.agrformet.2018.02.028.

Tillman, J.E., 1972. The indirect determination of stability, heat and momentum fluxes in the atmospheric boundary layer from simple scalar variables during dry unstable conditions. J. Appl. Meteorol. https://doi.org/10.1175/1520-0450(1972)011<0783:tidosh>2.0.co;2.

Wood, C.R., Lacser, A., Barlow, J.F., Padhra, A., Belcher, S.E., Nemitz, E., Helfter, C., Famulari, D., Grimmond, C.S.B., 2010. Turbulent Flow at 190 m height above London during 2006–2008 : A climatology and the applicability of similarity theory. Boundary-Layer Meteorol. 77–96. https://doi.org/10.1007/s10546-010-9516-x.

Wyngaard, J.C., Coté, O.R., Izumi, Y., 1971. Local free convection, similarity, and the budgets of shear stress and heat flux. J. Atmos. Sci. 28, 1171–1182 (doi.10.1175/1520-0469(1971)028<1171:lfcsat>2.0.co;2).

Yadav, J.S., Roubin, G.S., King, P., Iyer, S., Vitek, J., 1996. Angioplasty and stenting for restenosis after carotid endarterectomy: initial experience. Stroke 27, 2075–2079. https://doi.org/10.1161/01.STR.27.11.2075.